Mon. Not. R. astr. Soc. (1969) **142**, 295–316.

AN ANALYSIS OF THE CEPHEID VARIABLE RT AURIGAE

*M. K. V. Bappu and Nirupama Raghavan**

(Received 1968 August 15)

Summary

High dispersion spectra of the cepheid variable RT Aurigae have been used for an analysis of the parameters of the stellar atmosphere over a cycle of pulsation. Eighteen of these spectra were utilized for a study of the radial velocities. The displacement curve derived from the velocities was utilized with the light and colour curves of Eggen, Gascoigne & Burr to furnish by the application of Wesselink's method, a value of $R/R_\odot = 33{\cdot}7$. A differential curve of growth analysis relative to the Sun has been carried out at eleven phases to evaluate the variation of the atmospheric parameters. The range in θ_{exc} is from 0·94 to 1·07. The variation of $\rho\kappa$ is by a factor of ten over the cycle. A second hump in this curve at phase 0·68 P is perhaps a result of the sudden onset of a pulse of compression. Mean abundances relative to [Fe] have been derived for 21 elements. A general deficiency in s-process elements is seen in comparison with those formed by the e-process.

1. *Introduction.* RT Aurigae is one of the short period classical cepheids of the northern hemisphere that is bright enough to permit a high dispersion study of the stellar atmosphere over a pulsation cycle. Discovered as a light variable of the cepheid class by Astbury in 1905, with subsequent light curves by Kukarkin (1935) and Bennett (1941), the most recent observations of light variations by Eggen, Gascoigne & Burr (1957) show no necessity of a revision in the value of the period of 3·728261 days derived by Kukarkin. Velocity curves for this star have been measured by Duncan (1908) and Petrie (1932). The light curve is typical of Eggen's type A cepheids and there is very little difference between phase of maximum light and phase of maximum velocity of approach. An anomalously large colour and light amplitude for its period led Eggen, Gascoigne & Burr to speculate on the possibility of RT Aurigae being a Population II cepheid, despite its low galactic latitude and indistinguishable differences of characteristics from the classical cepheids.

2. *The radial velocities.* Eighteen spectrograms obtained with the 100-in. telescope in the years 1951 and 1952 were measured for radial velocity. Six of these spectrograms were obtained with the 73-in. camera yielding a dispersion of 4·5 Å mm^{-1} while the remaining spectra are of 10 Å mm^{-1} dispersion. The phases were calculated with Kukarkin's ephemeris:

$$\text{Phase} = \frac{JD - 2\,420\,957{\cdot}466}{3{\cdot}728261}.$$

The photoelectric observations of Eggen *et al.* which cover the epoch of our spectrograms do not demonstrate any need of a change in period. Our radial velocity measures form Table I. We could detect no systematic velocity differences

* Present address: Department of Physics, Indian Institute of Technology, Kanpur.

TABLE I

Radial velocities of RT Aurigae

λ	Element	Radial velocity for each coudé plate								
		Ce 7970	Ce 7700	Ce 7739	Ce 7655a	Ce 7661	Ce 8329	Ce 7665a	Ce 8313	Ce 7750
4028·33	Ti II	2·0	3·0	3·5	12·2	13·1	13·9	24·6	23·0	26·8
4084·50	Fe I	4·7	0·1	3·7	7·8	7·9	12·1	23·8	20·8	24·6
4118·55	Fe I	4·5	—	1·7	8·7	—	11·6	23·8	20·0	25·6
4139·93	Fe I	—	—	1·7	—	6·6	13·2	—	20·9	24·2
4174·92	Fe I	6·3	4·0	2·5	6·7	8·9	11·1	23·8	20·1	23·3
4178·85	Fe II	4·1	2·5	1·9	10·3	9·6	13·4	24·5	22·3	26·7
4187·04	Fe I	5·5	4·7	5·1	7·4	10·4	12·4	23·7	21·0	—
4206·70	Fe I	—	3·3	2·5	5·3	8·2	11·2	20·8	19·8	25·6
4233·61	Fe I	−0·6	−1·0	4·3	4·7	9·8	12·6	21·5	21·4	26·0
4250·79	Fe I	5·8	4·1	4·0	7·6	9·8	12·3	20·8	22·6	25·6
4267·83	Fe I	5·7	—	4·2	7·7	12·0	9·5	19·4	20·5	24·8
4271·16	Fe I	3·5	4·9	2·0	7·0	8·4	11·4	20·8	21·3	24·2
4273·32	Fe II	3·5	9·2	7·4	10·6	13·5	16·8	28·0	24·9	29·5
4290·93	Ti I	2·0	6·3	2·0	—	—	10·6	21·5	20·5	24·6
4296·57	Fe II	6·2	7·0	7·9	11·3	12·8	15·9	25·8	26·1	29·7
4303·17	Fe II	4·0	4·9	5·1	9·2	9·2	12·5	21·9	21·2	24·8
4312·86	Ti II	3·3	1·3	4·8	7·8	9·2	13·5	20·8	24·5	26·7
4330·71	Ti II	3·9	−1·4	5·0	7·9	8·6	13·9	—	21·6	25·0
4375·93	Fe I	5·0	2·9	4·0	7·3	10·8	12·7	22·9	23·6	25·9
4387·90	Fe I	2·8	—	7·0	6·6	—	13·7	25·7	22·9	27·6
4388·41	Fe I	2·1	—	4·2	10·1	—	11·6	20·8	20·9	25·2
4394·06	Ti II	2·8	5·7	5·2	6·7	10·1	12·5	18·7	—	25·5
4395·85	Ti II	3·5	2·9	6·1	8·0	8·8	12·2	21·5	22·0	25·8
4404·75	Fe I	7·6	5·0	5·1	9·5	11·6	—	25·7	22·5	28·1
4416·82	Fe II	6·8	3·0	4·5	7·4	10·2	12·3	23·6	23·6	26·5

4417·82	Ti II	2·6	2·3	3·0	6·7	9·5	12·9	22·2	21·2	25·8
4421·95	Ti II	6·1	2·3	5·1	6·1	12·3	11·6	22·9	22·3	25·8
4430·62	Fe I	3·3	4·4	5·1	6·8	12·3	13·5	22·9	22·1	25·4
4433·22	Fe I	4·6	5·1	6·0	6·8	9·5	12·0	19·4	21·1	26·6
4442·34	Fe I	4·6	5·8	5·3	7·5	11·6	13·0	24·3	22·5	23·2
4447·72	Fe I	3·8	5·1	5·9	11·0	13·1	11·7	20·8	22·1	26·8
4466·55	Fe I	5·0	3·7	4·4	7·6	11·6	11·2	22·2	21·6	25·2
4491·40	Fe II	5·0	6·5	4·9	8·3	11·7	13·1	25·6	22·1	29·8
4494·57	Fe I	4·9	3·1	3·7	8·3	9·0	11·0	18·1	20·7	24·1
4508·28	Fe II	4·8	3·8	4·9	8·4	10·4	11·9	—	21·9	25·8
4515·34	Fe II	4·1	4·5	5·7	7·7	7·7	11·1	21·5	20·1	25·4
4520·23	Fe II	—	5·2	4·5	7·1	11·1	11·1	21·5	20·8	25·7
4534·78	Ti I	8·0	—	6·6	—	—	12·6	20·1	20·6	24·1
4547·85	Fe I	—	6·6	—	8·5	—	13·0	20·8	20·3	26·9
4602·95	Fe I	4·3	6·6	—	7·3	10·6	12·8	20·1	22·1	—
4620·50	Fe II	6·9	4·6	—	10·7	8·0	12·3	22·8	21·2	—
4625·05	Fe I	4·2	2·6	—	8·7	5·3	10·0	20·1	19·4	—
4632·92	Fe I	—	2·6	—	10·7	5·4	11·2	20·1	19·9	—
4635·33	Fe II	—	—	—	—	—	12·3	—	20·0	—
4636·35	Ti II	— —	—	—	—	—	—	—	20·8	—
4638·02	Fe I	2·1	—	—	6·7	—	12·9	21·5	21·3	—
4647·44	Fe I	4·7	—	—	—	—	11·8	18·2	22·0	—
4233·19	Fe II	3·0	1·9	2·4	3·2	8·3	11·0	22·3	—	—
4199·97	Fe I	2·5	—	2·5	3·8	6·8	11·8	20·1	20·3	24·7
4418·34	Ti II	2·6	7·1	5·4	6·0	9·5	12·3	20·8	21·7	25·6
Phase		0·024	0·046	0·086	0·107	0·178	0·215	0·370	0·414	0·433

TABLE I (*continued*)

λ	Element	Radial velocity for each coudé plate								
		Ce 7532	Ce 7535a	Ce 8319	Ce 7969a	Ce 7996	Ce 7543a	Ce 7543b	Ce 7546	Ce 8323
4028·33	Ti II	—	35·3	40·5	39·0	—	35·3	33·7	34·4	6·5
4084·50	Fe I	29·3	33·8	38·0	36·7	—	33·8	29·9	27·5	7·5
4118·55	Fe I	—	38·2	—	38·3	—	36·7	40·3	37·2	6·0
4139·93	Fe I	24·2	33·7	37·8	38·1	37·9	35·9	29·9	26·8	7·4
4174·92	Fe I	30·1	32·2	37·4	37·5	39·5	33·6	30·6	30·5	6·9
4178·85	Fe II	26·4	34·4	38·4	35·3	38·8	34·4	35·0	31·2	8·5
4187·04	Fe I	27·9	35·1	38·3	36·6	—	32·2	30·6	29·0	6·3
4206·70	Fe I	28·6	30·7	37·9	37·1	—	32·9	32·8	29·0	6·1
4233·61	Fe I	27·9	31·4	40·1	33·1	40·2	34·3	28·4	27·6	7·9
4250·79	Fe I	—	32·8	26·4	42·9	40·6	35·7	31·3	29·0	7·6
4267·83	Fe I	24·3	30·7	37·5	40·0	42·7	34·2	29·8	30·5	10·5
4271·16	Fe I	27·2	29·2	26·7	34·0	42·5	34·2	32·7	30·4	7·0
4273·32	Fe II	—	34·9	42·2	41·8	45·3	39·2	36·3	34·7	8·3
4290·93	Ti I	34·3	29·2	36·5	—	—	36·4	32·0	29·0	4·6
4296·57	Fe II	35·6	33·5	42·7	40·8	47·0	39·2	36·2	31·9	8·7
4303·17	Fe II	32·2	28·5	39·6	39·3	—	34·9	33·4	30·4	7·5
4312·86	Ti II	29·3	32·0	37·7	34·9	41·9	34·2	30·5	27·6	7·5
4330·71	Ti II	28·6	—	37·9	43·0	—	—	29·8	—	7·3
4375·93	Fe I	30·7	32·7	38·4	39·0	44·5	36·9	33·3	31·1	7·2
4387·90	Fe I	30·0	31·3	38·1	38·1	38·7	29·2	34·7	31·8	6·0
4388·41	Fe I	29·3	32·0	39·3	33·2	43·6	34·1	30·5	29·0	9·7
4394·06	Ti II	27·9	32·7	36·8	—	38·6	32·7	29·8	29·0	6·6
4395·85	Ti II	32·8	29·9	37·9	37·3	40·1	35·5	32·6	29·0	7·6
4404·75	Fe I	32·8	32·7	41·0	38·6	41·9	35·4	32·6	33·2	7·0
4416·82	Fe II	27·2	31·3	38·6	37·9	38·9	35·4	31·2	31·8	7·1

4417·82	Ti II	26·5	32·0	37·7	37·0	37·6	34·7	33·9	31·8	5·9
4421·95	Ti II	27·9	32·0	38·3	38·3	43·1	38·3	31·9	30·4	7·1
4430·62	Fe I	27·9	32·0	38·0	35·5	40·2	33·3	31·2	30·4	7·4
4433·22	Fe I	29·3	32·0	37·4	35·4	—	34·0	33·9	31·8	8·1
4442·34	Fe I	32·1	30·6	38·5	36·7	38·6	36·8	34·6	29·7	8·9
4447·72	Fe I	30·7	31·9	38·8	37·9	42·7	36·8	33·2	29·7	8·9
4466·55	Fe I	28·6	31·2	37·6	37·1	41·1	34·7	31·8	30·4	6·7
4491·40	Fe II	32·0	33·3	39·0	39·5	31·4	36·0	37·9	29·7	8·0
4494·57	Fe I	26·5	30·5	37·8	34·6	40·7	31·9	29·8	26·9	7·4
4508·28	Fe II	28·6	32·6	38·7	36·5	41·2	34·6	34·5	30·3	7·8
4515·34	Fe II	27·9	29·2	35·9	39·1	41·1	33·9	32·5	28·3	7·5
4520·23	Fe II	28·6	30·5	36·6	38·3	41·0	36·6	32·5	29·6	6·9
4534·78	Ti I	30·0	29·8	36·8	41·5	41·5	34·2	—	27·6	—
4547·85	Fe I	28·6	—	37·4	35·9	45·3	—	—	29·0	9·4
4602·95	Fe I	28·6	32·5	38·1	36·6	41·9	34·5	33·1	31·0	8·1
4620·50	Fe II	26·9	30·5	39·8	37·1	36·4	34·5	35·0	32·3	8·8
4625·05	Fe I	24·6	29·2	42·7	33·7	36·3	29·8	—	26·8	9·4
4632·92	Fe I	27·3	28·5	37·4	—	32·9	35·1	—	30·3	—
4635·33	Fe II	—	—	38·9	—	—	—	—	—	10·3
4636·35	Ti II	—	—	38·0	—	—	—	—	—	—
4638·02	Fe I	—	—	39·8	—	—	—	—	32·9	9·7
4647·44	Fe I	26·9	29·8	38·0	38·6	—	35·1	33·7	27·6	9·2
4233·19	Fe II	27·3	30·0	—	36·0	40·2	—	37·1	—	—
4199·97	Fe I	27·9	30·7	36·7	35·7	39·9	29·2	31·3	28·3	6·7
4418·34	Ti II	30·0	31·3	37·7	37·7	41·1	36·8	36·7	31·8	6·5
Phase		0·565	0·587	0·680	0·750	0·825	0·834	0·838	0·861	0·946

between the Fe I and Fe II values as a function of excitation potential. However, when we divided the measured lines into two categories on the basis of the atmospheric heights in the solar chromosphere as given by Mitchell (1930) we notice a velocity difference between the 'high' and 'low' level lines that is a function of phase. The two categories comprised the height ranges 350–800 km and 850–1200 km. This apparent level effect can be seen in Table II where we give the average velocity for each phase for the mean heights covering the two ranges. This agrees well with Petrie's earlier finding of the same characteristic.

TABLE II

Phase	Radial velocities Mitchell height criterion			Phase	Radial velocities Mitchell height criterion		
	Low	High	'Selected'		Low	High	'Selected'
0·024	4·15 (22)	4·23 (12)	4·46 (12)	0·565	28·99 (25)	28·71 (13)	28·45 (19)
0·046	4·03 (19)	3·38 (13)	4·14 (12)	0·587	31·29 (23)	31·66 (13)	31·06 (17)
0·086	4·35 (20)	4·22 (13)	4·04 (14)	0·680	38·47 (29)	38·41 (12)	38·51 (19)
0·107	7·88 (22)	7·73 (13)	7·71 (15)	0·750	37·00 (22)	36·89 (13)	36·87 (15)
0·178	9·48 (20)	9·84 (13)	9·17 (13)	0·825	40·08 (18)	40·87 (11)	40·60 (11)
0·215	12·31 (29)	12·32 (12)	12·11 (19)	0·834	34·50 (24)	34·73 (13)	35·29 (17)
0·370	21·43 (23)	22·55 (12)	21·09 (18)	0·838	32·13 (21)	32·39 (13)	31·85 (14)
0·414	21·09 (27)	21·95 (13)	20·82 (19)	0·861	30·18 (27)	30·02 (13)	30·02 (20)
0·433	25·22 (21)	25·97 (12)	25·01 (15)	0·946	7·91 (25)	7·24 (13)	8·06 (17)

If such a level effect indicates different heights of origin in the atmosphere of the cepheid for the different lines, it will be necessary to restrict the study of the displacement with phase, as derived from the velocity curve, to a narrow height range. In doing so one uses the chromospheric heights of Mitchell only as an aid to limit the selection of lines in a distended atmosphere without any assumption whatsoever regarding the identity of the cepheid atmosphere and the solar chromosphere. We have, therefore, averaged in Table II radial velocity measures of RT Aurigae from 'selected' lines that have solar chromospheric heights in the range 350–700 km. A velocity curve from these 'selected' lines can be seen in Fig. 1. The velocities were evaluated at 50 phases from this curve. These velocities are reduced first to take into account the velocity of the star as a whole. The surface velocity is determined next from the radial velocity, assuming a limb darkening coefficient of 0·6. The displacements can then be evaluated by numerical integration. We choose the integration constant suitably so that the time average of the displacements $r-R$ is zero, in accordance with the definition of R as the mean radius. Table III gives the values of surface velocity, dr/dt and $r-R$ for the 50 phases. Plots of these parameters can be seen in Fig. 2.

We employ the light and colour curves of Eggen, Gascoigne & Burr (1957) in combination with the displacements calculated above to determine the radius of the cepheid following Wesselink (1946). From six selected equal-colour phase

values, we derive a mean value of the radius as $R_{\text{RT Aur}} = 33{\cdot}7\ R_{\odot}$ or $234{\cdot}6 \times 10^{10}$ cm.

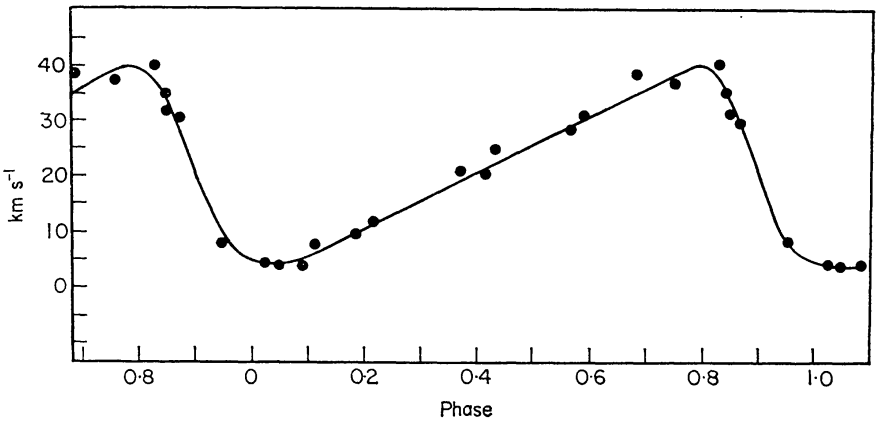

FIG. 1. *The velocity curve of RT Aurigae.*

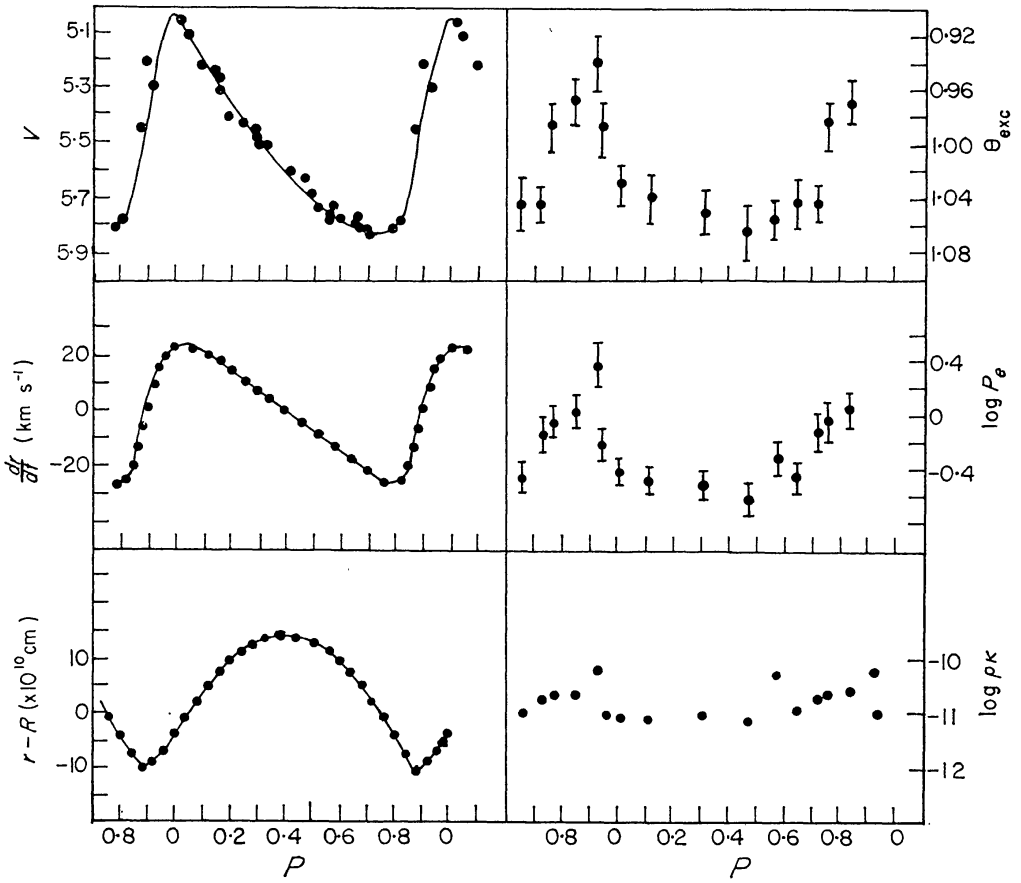

FIG. 2. *The variation over a cycle of some of the physical parameters of RT Aurigae.*

3. *The photometric reductions.* Eleven spectrograms taken at representative phases were used for the measurement of equivalent widths. All the plates cover the wavelength range 3900–4700 Å and are well exposed for spectrophotometry. Four of these plates were obtained with the 73-in. camera on baked IIa–o plates, the rest being spectra obtained with the 32-in. camera on unbaked IIa–o emulsion.

Exposure times for the 4·5 Å mm^{-1} dispersion plates were 120 min. The 10 Å mm^{-1} plates had exposure times of about 40 min. In addition to the usual step-slit calibration that can be impressed on the plate simultaneously with the star spectrum, calibration spectrograms obtained with a wedge slit spectrograph in the 100-in. dome were developed simultaneously with the stellar spectrograms. Nine of these spectra were traced with the Babcock direct intensity microphotometer, the step-slit calibration being used to evaluate the zero of the intensity scale. Equivalent widths from these tracings were derived after planimetry along the profiles of the lines selected for measurement. For the two remaining spectra we determined equivalent widths by the triangle approximation, after establishing over a range of W values the relation between the exactly measured W and the area of the triangle drawn to represent the line contour. The continuum drawn on each tracing is a smooth curve that passes through successive line-free windows. We have log W/λ measures of the selected Fe I and Fe II lines for all eleven phases. These are given in Table IV. Lines of other elements used principally for abundance determinations have been measured on only the four 73-in. camera plates for four phases that are well distributed over the light curve. These values of log W/λ are presented in Table V.

4. *The curve of growth analysis.* The range in spectral variation of RT Aurigae is from spectral class F5·5Ib to GoIb. We, therefore, adopt the technique of a differential curve of growth analysis relative to the Sun in order to derive the atmospheric parameters. With solar equivalent widths given in the *Utrecht Photometric Catalogue of Fraunhofer lines*, we have obtained the log $\eta_\odot$ data from the Goldberg–Pierce solar curve of growth as published by Aller (1953). We then have, in the conventional notation employed today for such analyses

$$\log \eta_* = \log \eta_\odot + \chi(\theta_{\rm exc}{}^\odot - \theta_{\rm exc}{}^*) + [N/\kappa V]$$

wherein log η_* for each line is expressed in terms of the solar log η value, a Boltzmann correction for the excitation temperature inequality between Sun and cepheid, and a constant for each ion that involves the abundances, opacities and Doppler parameters of both Sun and the star. In constructing the curve of growth for each phase we adopted a trial value of $\theta_{\rm exc}{}^*$ and formed log η_*. On a plot of log W/λ against log η_* a Milne–Eddington curve of growth computed by Wrubel (1949) with $B^0/B^1 = \frac{1}{3}$ was made to yield the best fit through the points. Then for each observed log W/λ, we obtained from the theoretical curve of growth a value of log η_* (obs). For each line we now have

$$\Delta\eta = \log \eta_*(\text{obs}) - \log \eta_\odot = \text{const.} + \chi . \Delta\theta$$

where $\Delta\theta = \theta_{\rm exc}{}^\odot - \theta_{\rm exc}{}^*$. We then evaluate $\Delta\theta$ by a least squares solution and use it in our next trial. This process is repeated iteratively until the assumed and calculated values agree with each other. The Fe I lines used have values of excitation potential of the lower levels ranging from 0·05 to 3·9 eV. We have preferred to use the above method of evaluating $\theta_{\rm exc}$ to the usual one of visual inspection of the best values that minimize systematic differences in log η between the high and low excitation lines. The uncertainty in the determination of $\theta_{\rm exc}$ is less than $\pm$0·03. These plots of log W/λ vs log η_* are represented in Fig. 3. The solid line is the theoretical curve of growth. The variation of $\theta_{\rm exc}{}^*$ with phase can be seen in Fig. 2. The vertical bars denote the standard error for each

determination. The horizontal and vertical displacements of the theoretical curves of growth yield $[V]$ and $[N_{\text{Fe I}}/\kappa V]$.

5. *The determination of electron pressure and opacity.* There is sufficient evidence from analyses by Greenstein (1948), Kraft *et al.* (1959) and Abt (1960) that one can in the case of *F*-type stars assume $\theta_{\text{ion}} = \theta_{\text{exc}} - 0{\cdot}15$. We assume this relation to apply in the case of RT Aurigae. The shifts of the Fe II lines seen on Fig. 3 with respect to the Fe I curve of growth, yield [Fe II/Fe I]. A straight mean of these shifts for all Fe II lines measured at each phase gives the mean value of [Fe II/Fe I]. With the assumed value of θ_{ion} and the log Fe II/Fe I value in the solar case (1·0 at $\bar{\tau} = 0{\cdot}35$), we proceed to determine log P_e from the Saha equation.

Gingerich (1962) has tabulated as a function of θ_{ion} the contributions to opacity from the negative hydrogen ion and to Rayleigh scattering and bound–free absorption by neutral hydrogen. This enables us to evaluate for each phase the total absorption coefficient per gram of stellar material

$$\kappa = \kappa(H^-).P_e + \kappa(H)$$

From Aller's (1963) compilation of gas pressure P_g as a function of θ_{ion} and P_e for a solar like abundance we obtain the gas pressure for each phase of RT Aurigae. From the perfect gas law we derive the value of ρ the density for each phase. Following the reasoning of Schwarzschild, Schwarzschild & Adams (1948) we have tabulated log $\rho\kappa$ in Table VI along with the other derived parameters for each phase of RT Aurigae. Fig. 2 also shows plots of log P_e and log $\rho\kappa$. We find

TABLE III

Phase	dr/dt (km s^{-1})	$r-R$ (10^{10} cm)	Phase	dr/dt (km s^{-1})	$r-R$ (10^{10} cm)
0·015	+23·50	−7·398	0·515	− 8·64	+ 7·685
0·035	+23·65	−5·876	0·535	−10·05	+ 7·084
0·055	+23·50	−4·353	0·555	−11·60	+ 6·487
0·075	+22·94	−2·852	0·575	−13·16	+ 5·699
0·095	+21·95	−1·403	0·595	−14·57	+ 4·806
0·115	+20·68	−0·028	0·615	−15·98	+ 3·823
0·135	+19·27	+1·259	0·635	−17·53	+ 2·742
0·155	+17·86	+2·455	0·655	−18·94	+ 1·567
0·175	+16·45	+3·537	0·675	−20·35	+ 0·300
0·195	+14·76	+4·539	0·695	−21·76	− 1·058
0·215	+13·35	+5·444	0·715	−23·03	− 2·499
0·235	+11·94	+6·260	0·735	−24·44	− 4·028
0·255	+10·39	+6·979	0·755	−25·85	− 5·653
0·275	+ 8·84	+7·597	0·775	−26·83	− 7·363
0·295	+ 7·43	+8·123	0·795	−26·55	− 9·095
0·315	+ 5·88	+8·550	0·815	−25·14	−10·805
0·335	+ 4·47	+8·883	0·835	−19·50	−12·254
0·355	+ 3·06	+9·126	0·855	−12·87	−13·301
0·375	+ 1·65	+9·279	0·875	− 5·82	−15·212
0·395	+ 0·09	+9·356	0·895	+ 1·93	−15·085
0·415	− 1·45	+9·309	0·915	+ 9·83	−13·717
0·435	− 2·72	+9·179	0·935	+15·61	−12·882
0·455	− 4·41	+8·946	0·955	+19·98	−11·710
0·475	− 5·82	+8·616	0·975	+21·95	−10·349
0·495	− 7·23	+8·196	0·995	+22·94	− 8·848

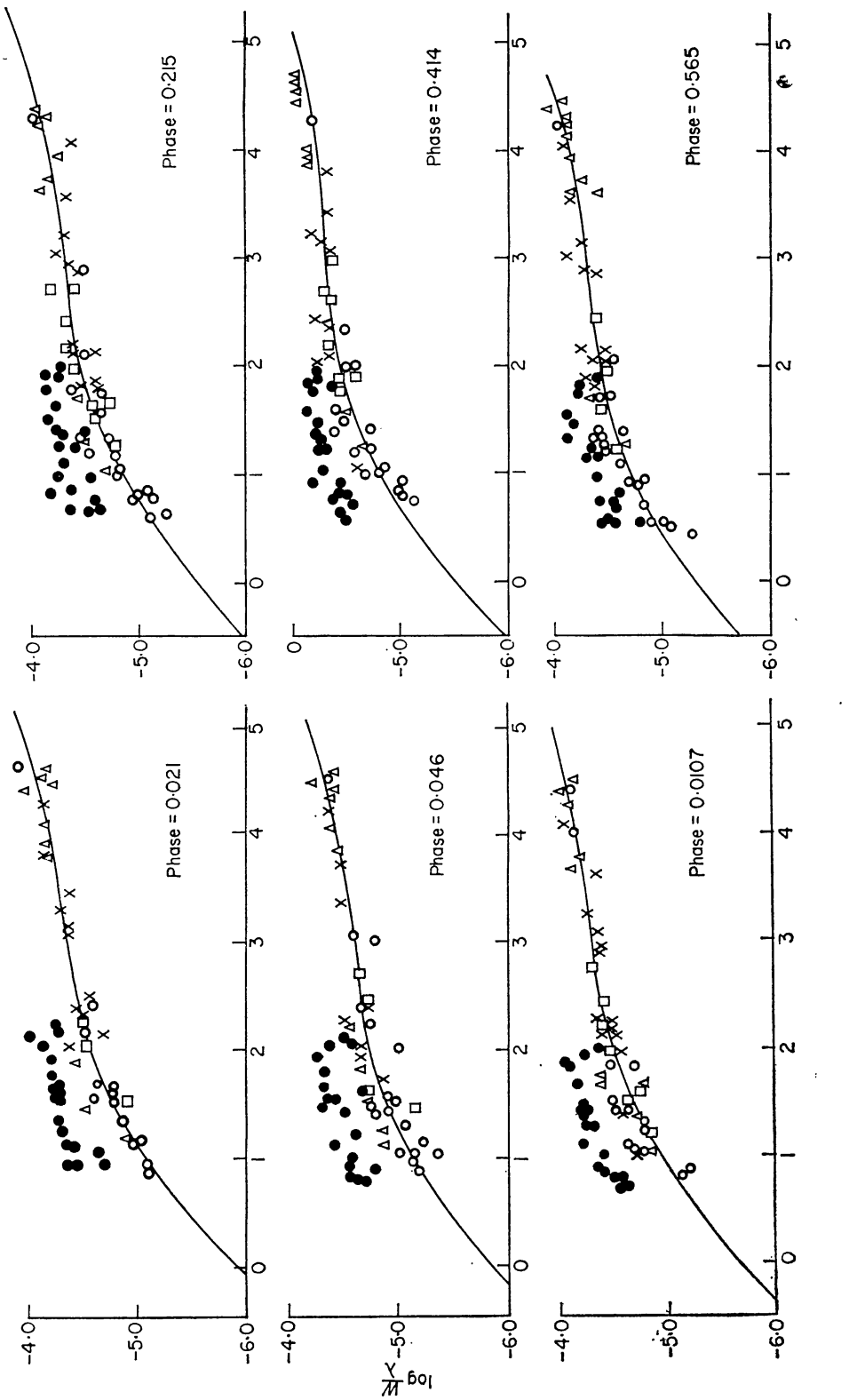

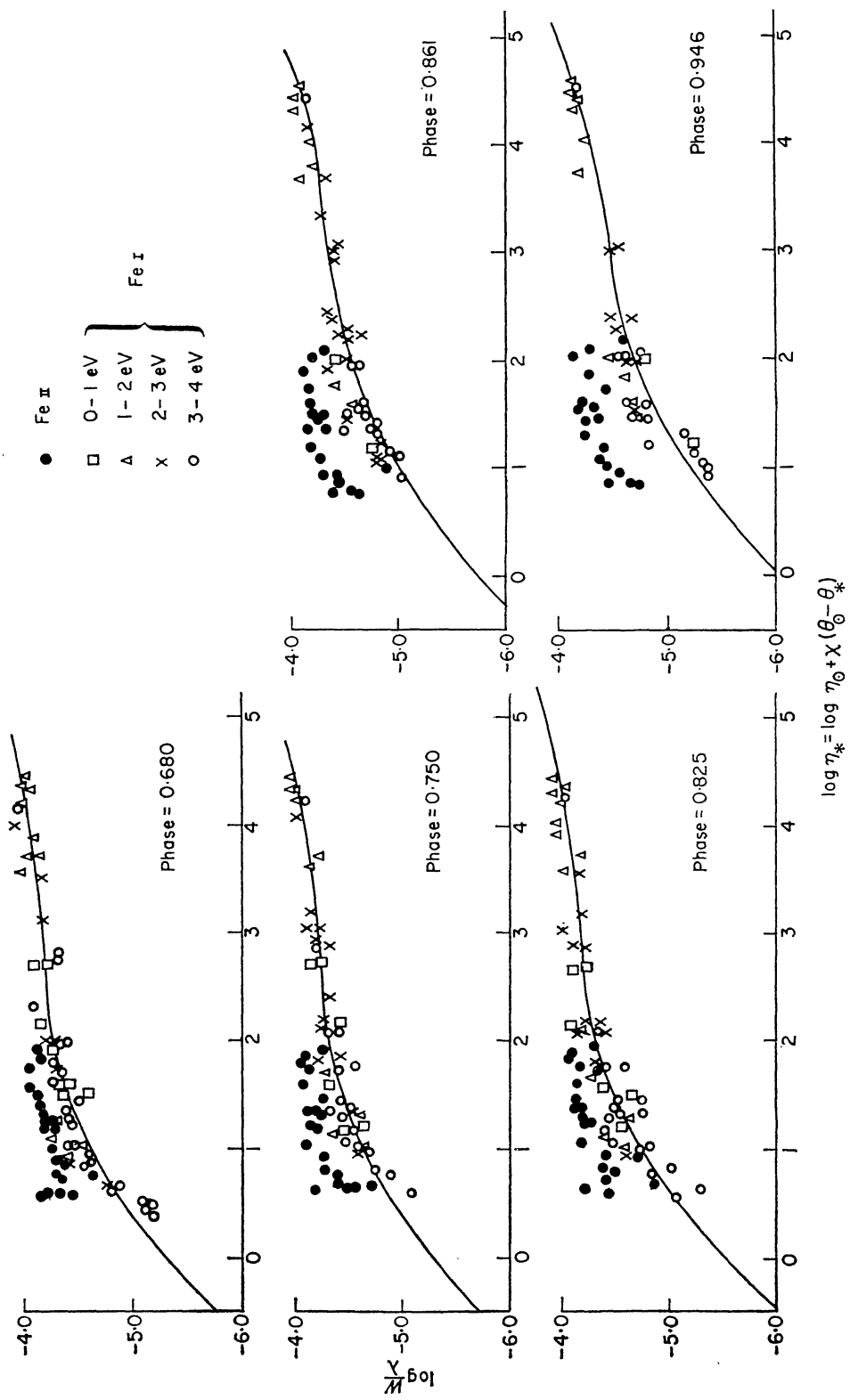

FIG. 3. *Curves of growth of RT Aurigae at different phases.*

TABLE IV(a)

Equivalent widths of Fe I

Wavelength	RMT No.	log η_0	$-\log W/\lambda$										
			0·024	0·046	0·107	0·215	0·414	0·565	0·680	0·750	0·825	0·861	0·946
4001·67	72	1·81	4·39	4·62	4·43	4·49	4·24	4·41	4·13	4·23	4·32	4·33	4·70
4044·61	359	2·20	4·56	4·64	4·49	4·38	4·28	4·37	4·20	4·56	4·41	4·34	4·66
4063·60	43	4·35	4·13	4·17	4·03	4·09	4·08	4·07	4·08	4·07	4·08	4·08	4·12
4071·74	43	4·27	3·90	4·40	4·13	4·04	4·02	4·15	3·93	3·93	4·06	4·09	4·18
4072·52	698	1·30	4·53	4·68	4·73	4·52	4·50	4·81	4·34	4·62	4·63	4·77	4·74
4079·85	359	1·85	4·75	4·65	4·57	4·60	4·36	4·50	4·28	4·43	4·49	4·52	4·75
4112·35	695	1·33	4·78	4·85	4·89	4·74	—	4·77	4·52	4·55	4·76	4·69	4·81
4139·93	18	1·63	5·17	—	4·79	4·73	4·59	—	4·41	4·68	4·76	—	4·88
4143·87	43	3·93	4·19	4·34	4·20	4·28	4·16	4·25	4·09	4·29	4·00	4·16	4·26
4147·67	42	2·13	4·48	4·56	4·42	—	4·35	4·41	4·22	4·35	4·23	4·30	4·48
4174·94	19	1·94	4·57	4·70	4·48	4·40	4·35	4·25	4·26	4·40	4·35	4·54	4·82
4175·64	354	2·10	4·44	4·49	4·47	4·41	4·36	4·58	4·26	4·30	4·34	4·48	4·54
4187·04	152	3·10	4·37	4·44	4·29	4·33	4·32	4·62	4·18	4·16	4·21	4·26	4·39
4191·44	152	3·03	4·27	4·34	4·37	4·24	4·18	4·37	3·99	4·12	4·05	4·12	4·71
4199·97	3	1·50	4·92	4·20	4·69	4·60	4·46	4·23	4·37	4·66	4·68	—	4·96
4202·03	42	3·61	4·19	4·20	4·17	4·15	4·16	4·82	3·96	4·19	4·05	4·12	4·21
4206·70	3	2·41	4·58	4·94	4·44	4·35	4·33	4·27	4·23	4·33	4·39	4·53	4·79
4233·61	152	3·55	4·14	4·73	4·34	4·35	4·32	4·49	4·19	4·19	4·19	4·34	4·38
4250·79	42	3·74	4·17	4·43	4·23	4·20	4·20	4·27	5·16	4·26	4·21	4·23	4·34
4260·48	152	4·04	4·15	4·33	4·08	4·42	4·18	4·37	3·90	4·02	3·97	4·15	4·25
4265·26	993	1·48	5·06	5·38	4·84	4·87	4·77	—	4·81	4·92	4·76	—	5·49
4267·83	482	2·09	4·60	—	4·54	4·50	4·42	4·66	4·36	4·42	4·37	4·59	4·84
4271·76	42	4·24	3·98	4·37	4·11	4·08	4·07	4·25	3·98	4·03	4·02	4·03	4·15
4276·68	976	1·03	5·06	5·13	4·67	4·81	4·73	—	4·61	5·24	4·83	—	5·19
4304·55	414	2·10	4·92	—	4·78	4·59	4·49	4·61	4·41	4·42	4·45	4·64	5·20

4365·91	415	0·83	5·06	—	5·21	5·10	4·88	—	4·98	—	5·02	—	—
4372·99	473	0·58	5·09	5·61	5·49	5·12	5·00	5·19	5·01	5·07	5·07	—	—
4377·38	990	0·53	—	—	—	—	5·14	5·38	5·17	—	—	—	—
4377·80	645	0·65	—	—	—	—	5·02	5·01	5·10	—	—	—	—
4383·55	41	4·45	4·19	4·37	4·17	4·07	4·04	4·23	4·00	3·94	3·98	4·08	4·14
4387·90	476	1·29	5·01	4·77	4·78	4·64	4·49	4·58	4·41	4·68	4·43	4·53	4·94
4389·24	2	1·21	5·24	5·16	4·81	4·79	4·59	5·12	4·58	4·61	4·56	4·76	5·27
4392·59	973	0·63	5·44	5·17	—	5·28	5·00	—	5·18	5·70	5·29	—	5·69
4404·75	41	4·30	4·23	4·39	4·15	4·16	4·06	4·22	3·98	4·02	3·98	4·12	4·19
4430·62	68	2·09	4·48	4·72	4·43	4·39	4·36	4·48	4·22	4·31	4·18	4·47	4·59
4432·57	797	0·80	5·04	5·35	—	5·11	4·82	—	4·87	4·75	—	—	5·34
4433·22	830	1·78	4·69	4·99	4·71	4·63	4·61	4·67	4·72	4·57	4·59	4·64	4·75
4439·88	116	0·80	—	—	—	5·01	4·53	4·98	4·31	—	—	—	5·64
4442·34	68	2·90	4·55	4·55	4·40	4·37	4·27	4·38	4·30	4·21	4·15	4·43	4·54
4447·72	68	2·87	4·33	4·76	4·38	4·44	4·34	4·49	4·21	4·34	4·27	4·42	4·50
4466·55	350	2·20	4·34	4·65	4·36	4·37	4·23	4·57	4·42	4·28	4·25	4·32	4·48
4485·68	830	1·17	4·78	4·77	4·77	4·78	4·41	4·73	4·33	4·57	4·49	4·77	4·82
4489·74	2	1·59	4·78	4·71	4·73	4·57	4·45	4·57	4·11	4·34	4·39	4·60	4·68
4517·53	472	0·99	4·88	5·25	4·80	4·82	4·59	4·82	4·54	4·71	4·74	5·00	4·85
4587·13	795	0·76	4·97	5·12	5·16	4·93	4·69	4·71	4·47	4·87	4·84	5·01	5·39
4602·00	39	1·02	4·89	5·86	4·84	4·73	4·69	4·94	4·55	4·65	4·60	4·88	5·25
4602·94	39	1·72	4·46	4·67	4·40	4·46	4·60	4·48	4·32	4·29	4·30	4·44	4·59
4611·28	826	1·76	4·52	4·88	4·48	4·40	4·59	4·54	4·30	4·43	4·44	4·58	4·59
4619·29	821	1·18	4·61	4·91	4·60	4·67	4·72	—	4·44	4·45	4·40	4·49	4·70
4625·05	554	1·35	4·65	4·73	4·54	4·54	4·40	4·57	4·44	4·32	4·56	4·52	4·64
4630·12	115	0·98	—	—	4·65	—	—	4·88	4·39	4·61	4·58	4·81	—
4637·51	554	1·39	—	4·80	4·63	—	—	4·55	4·40	4·53	4·51	4·61	—
4638·02	822	1·44	—	—	4·52	—	—	4·88	4·40	4·45	4·54	4·63	—
4643·47	820	1·06	—	5·06	4·62	—	—	4·50	4·42	4·34	4·49	4·92	—
4647·44	409	1·37	—	4·89	4·54	—	—	4·52	4·25	4·28	4·36	4·53	—

TABLE IV(b)

Equivalent widths of Fe II

Wavelength	RMT No.	log $\eta_\odot$	$-\log W/\lambda$										
			0·024	0·046	0·107	0·215	0·414	0·565	0·680	0·750	0·825	0·861	0·946
4002·07	29	0·65	4·45	4·66	4·56	4·64	4·45	4·71	4·45	4·50	4·45	4·56	4·68
4128·74	27	0·94	4·45	4·61	4·44	4·56	4·43	4·67	4·37	—	4·73	4·45	4·68
4178·86	28	1·49	4·20	4·31	4·22	4·17	4·23	4·31	4·13	4·28	4·13	4·18	4·45
4233·17	27	1·78	4·11	4·22	4·10	4·16	4·18	—	4·06	4·13	4·20	4·14	4·64
4273·32	27	1·96	4·25	4·57	4·39	4·30	4·24	4·58	4·17	4·28	4·32	4·34	4·64
4296·57	28	1·62	4·20	4·31	4·18	4·23	4·14	4·25	4·05	4·10	4·15	4·18	4·28
4303·17	27	1·89	4·22	4·34	4·23	4·29	4·24	4·36	4·15	4·12	4·11	4·20	4·29
4369·40	28	0·73	4·63	4·77	4·55	4·52	4·57	4·69	4·34	4·42	—	4·43	4·57
4413·60	32	0·65	4·70	4·52	4·60	4·52	4·49	4·59	4·32	4·51	4·44	4·60	4·72
4416·82	27	1·37	4·28	4·41	4·29	4·51	4·29	4·59	4·18	4·22	4·19	4·26	4·31
4472·92	37	0·64	4·35	4·61	4·29	4·36	4·32	4·60	4·18	4·18	4·23	4·38	4·46
4489·18	37	1·06	4·27	4·49	4·20	4·31	4·27	4·50	4·27	4·13	4·20	4·19	4·25
4491·40	37	1·24	4·28	4·39	4·25	4·42	4·34	4·54	4·18	4·18	4·22	4·33	4·38
4508·28	38	1·33	4·22	4·28	4·22	4·31	4·20	4·48	4·19	4·20	4·21	4·26	4·19
4515·34	37	1·38	4·23	4·33	4·21	4·25	4·19	4·26	4·16	4·13	4·15	4·21	4·21
4520·22	37	1·24	4·26	—	4·30	4·27	4·18	4·43	4·28	4·19	4·23	4·17	4·25
4576·33	38	0·96	4·30	4·40	4·40	4·25	4·42	4·74	4·29	4·27	4·41	4·26	4·44
4582·84	37	0·83	4·32	4·56	4·33	4·38	4·39	4·53	4·26	4·27	4·38	4·32	4·39
4583·83	38	1·83	4·00	—	4·07	4·38	4·15	4·35	4·31	4·05	4·08	—	4·13
4620·51	38	0·81	4·40	4·54	4·34	4·16	4·52	4·68	4·67	4·40	4·50	4·43	4·44
4635·33	186	0·69	—	—	4·52	—	—	4·92	4·17	4·73	4·86	4·90	—

TABLE V

Equivalent widths

Wavelength	RMT No.	log $\eta_\odot$	$-\log W/\lambda$ 0·215	0·414	0·680	0·946
Mg I						
4167·27	15	3·17	4·33	4·39	4·27	4·49
4571·10	1	1·66	4·73	4·44	4·48	5·05
Mg II						
4390·58	10	0·59	4·91	—	4·14	5·36
4428·00	9	0·02	4·75	4·66	4·71	5·27
4481·13	4	1·35	4·12	4·17	4·13	4·04
Si II						
4128·05	3	2·10	4·34	4·37	4·25	4·41
Ca I						
4226·73	2	4·77	4·02	3·91	3·94	4·04
4283·00	5	2·46	4·43	4·35	4·44	4·52
4302·53	5	2·92	4·31	4·21	4·12	4·36
4318·65	5	2·17	4·41	4·35	4·21	4·45
4355·10	37	1·77	4·69	4·66	4·54	4·79
4425·44	4	2·57	4·49	4·40	4·36	4·56
4435·69	4	2·32	4·38	4·22	4·28	4·57
4455·89	4	−0·04	4·35	4·32	4·38	4·55
4578·56	23	1·42	4·63	4·55	4·48	4·83
Sc II						
4246·83	7	2·96	4·18	4·16	4·13	4·26
4294·77	15	1·12	4·43	4·48	4·29	4·57
4325·01	15	2·32	4·20	4·15	4·08	4·24
4354·61	14	1·27	4·46	4·33	4·22	4·67
4374·46	14	2·00	4·27	4·36	4·30	4·28
4400·36	14	1·53	4·26	4·23	4·15	4·32
4415·56	14	1·64	4·29	4·27	4·45	4·46
4431·37	14	0·45	4·62	4·57	4·52	4·96
Ti I						
4286·01	44	2·30	4·73	4·84	4·44	5·24
4287·40	44	1·04	4·83	4·75	4·65	5·17
4290·93	44	1·16	4·55	4·40	4·26	5·02
4457·43	113	1·44	4·52	4·46	4·42	4·78
4465·81	146	0·49	5·35	5·11	4·91	5·72
Ti II						
4028·33	87	1·77	4·27	4·18	4·27	4·36
4163·63	105	3·08	4·21	4·21	4·19	4·23
4287·89	20	1·76	4·23	4·21	4·08	4·31
4300·75	41	2·94	4·03	3·91	3·96	4·14
4301·93	41	2·76	4·12	4·22	4·05	4·25
4312·86	41	2·74	4·18	4·13	4·08	4·21
4316·81	94	0·74	4·48	4·35	4·41	4·59
4330·26	94	0·68	4·44	4·41	4·20	4·49
4350·83	94	1·05	4·39	4·18	4·07	4·42
4394·06	51	1·35	4·31	4·23	4·28	4·35
4395·03	19	2·46	4·08	4·03	4·00	4·13
4395·85	61	1·14	4·36	4·29	4·20	4·44
4399·77	51	2·04	4·29	4·25	4·13	4·26
4411·94	61	0·84	4·59	4·47	4·32	4·74
4417·72	40	1·74	4·24	4·26	4·14	4·25

TABLE V (*continued*)

Wavelength	RMT No.	log η_o	$-\log W/\lambda$ 0·215	0·414	0·680	0·946
4418·34	51	1·19	4·39	4·42	4·36	4·46
4421·95	93	0·85	4·54	4·40	4·40	4·59
4443·80	19	2·40	4·28	4·17	4·12	4·21
4468·49	31	2·30	4·18	4·13	4·06	4·19
4501·27	31	2·23	4·21	4·12	4·09	4·16
4545·14	30	0·82	4·37	4·34	4·22	4·51
4563·76	50	2·22	4·22	4·21	4·07	4·14
4568·31	60	0·32	4·57	4·57	4·47	4·74
4609·26	39	−0·05	4·69	4·79	4·72	4·85
4636·35	38	0·31	—	—	4·60	—
V I						
4111·78	27	2·16	4·58	4·45	4·47	4·87
4379·24	22	2·05	4·71	4·59	4·54	5·30
4389·97	22	1·51	4·87	4·61	4·38	5·26
4406·64	22	1·38	5·15	4·69	4·74	—
V II						
4023·39	32	1·25	4·39	4·38	4·32	4·56
4036·78	9	0·56	4·66	4·55	4·59	4·76
4065·07	215	0·98	5·30	4·70	4·73	5·13
4178·39	25	0·39	4·54	4·54	4·52	4·86
4183·44	37	1·46	4·48	4·52	4·39	4·61
4232·06	225	1·13	4·90	4·85	4·72	5·24
4564·61	56	0·08	4·54	4·49	4·46	4·80
Cr I						
4254·36	1	3·73	4·27	4·21	4·21	4·36
4371·28	304	2·01	4·60	4·52	4·44	4·68
4545·96	10	1·31	4·67	4·56	4·48	4·90
4591·39	21	1·00	4·81	4·51	4·38	5·12
4616·14	21	1·34	4·64	4·50	4·49	4·92
Cr II						
4051·95	19	1·65	4·40	4·42	4·30	4·64
4207·35	26	0·96	4·56	4·44	4·30	4·68
4252·62	31	0·52	4·56	4·45	4·41	4·59
4278·15	161	0·80	4·40	4·51	4·33	4·57
4539·63	39	2·23	4·48	4·48	4·45	4·73
4555·02	44	0·62	4·51	4·44	4·42	4·50
4558·66	44	1·16	4·20	4·21	4·25	4·25
4588·82	44	1·03	4·37	4·37	4·27	4·29
4592·09	44	0·73	4·62	4·44	4·48	4·53
4616·69	44	0·59	4·51	4·51	4·45	4·59
4618·80	44	1·29	4·41	4·44	4·34	4·38
Mn I						
4034·49	2	3·12	4·30	4·27	4·13	4·46
4055·54	5	2·32	4·50	4·42	4·36	4·77
4059·39	29	1·11	5·21	4·83	4·87	5·61
4082·94	5	1·86	4·67	4·55	4·40	4·95
4502·22	22	0·91	5·09	4·86	4·72	5·12
Mn II						
4510·21	17	0·11	5·35	4·97	5·13	5·49

TABLE V (*continued*)

Wavelength	RMT No.	log $\eta_\odot$	$-\log W/\lambda$ 0·215	0·414	0·680	0·946
Co I						
4020·91	16	1·55	4·76	4·53	4·56	5·25
4110·53	29	1·80	4·61	4·32	4·25	4·93
4121·32	28	2·42	4·48	4·33	4·29	4·82
Ni I						
4331·60	52	0·98	5·19	4·55	4·53	—
4410·52	88	0·88	4·76	4·70	4·75	5·26
4551·24	236	0·24	4·69	4·94	4·87	—
Ni II						
4015·51	12	0·30	4·38	4·25	4·30	4·58
4192·07	10	0·40	4·87	4·75	4·83	5·23
4244·80	9	0·02	5·11	4·82	4·96	5·04
4362·10	9	0·44	4·89	4·71	4·77	4·89
Sr II						
4077·74	1	3·81	3·89	4·85	3·69	3·94
4215·52	1	3·31	3·98	3·94	3·89	4·06
Y II						
4177·54	14	1·62	4·28	4·01	4·09	4·20
4374·92	13	1·55	4·18	4·18	4·13	4·27
4398·02	5	0·84	4·47	4·39	4·38	4·73
Zr II						
4050·32	43	0·29	4·57	4·51	4·32	5·00
4150·97	42	0·78	—	4·42	4·35	4·74
4179·81	99	0·11	4·69	4·79	4·69	5·11
4208·99	41	0·84	4·46	4·43	4·32	4·58
4211·86	15	1·06	4·36	4·27	4·31	4·57
4317·32	40	0·05	4·73	4·62	4·68	5·36
4333·28	132	0·00	4·94	4·86	5·16	5·04
4379·76	88	0·38	4·84	4·61	4·56	4·74
4403·33	79	0·75	4·62	4·49	4·37	4·96
Ba II						
4166·00	4	−0·09	4·88	4·93	4·92	5·41
La II						
4086·72	10	0·75	4·59	4·62	4·22	4·77
4123·23	41	0·82	4·55	4·39	4·33	4·89
4238·38	41	0·72	4·46	4·47	4·32	5·01
4263·59	84	0·64	5·21	4·93	4·91	5·21
4286·97	75	1·55	4·55	4·56	4·52	5·00
4322·51	25	−0·43	4·91	4·81	4·79	5·33
4333·76	24	0·54	4·46	4·36	4·24	4·53
Ce II						
4073·48	4	0·24	4·74	4·74	4·53	5·33
4083·28	60	0·43	4·76	4·69	4·56	5·23
4120·83	112	0·06	5·01	4·74	4·69	5·44
4186·60	10	1·87	4·49	4·52	4·44	4·77
4248·68	1	1·53	4·70	4·57	4·62	—
4382·14	2	−0·16	4·94	4·62	4·75	5·38
4562·36	1	0·16	4·67	4·58	4·52	5·00

TABLE V (*continued*)

Wavelength	RMT No.	log $\eta_\odot$	$-\log W/\lambda$ 0·215	0·414	0·680	0·946
Pr II						
4062·82	26	0·08	4·84	4·56	4·42	—
4222·98	4	−0·06	4·71	4·57	4·51	5·52
Nd II						
4061·12	10	1·05	4·66	4·56	4·42	4·96
4109·47	10	0·70	4·57	—	4·35	4·82
4303·57	10	1·03	4·61	4·50	4·34	4·92
4358·17	10	0·64	4·72	4·79	4·69	4·96
4462·98	6	0·04	4·75	4·65	—	5·31
Sm II						
4424·34	45	−0·18	4·63	4·49	4·60	5·18
4434·32	36	0·12	4·81	4·60	4·68	5·19
4457·37	7	−0·14	4·92	4·66	—	5·24
Eu II						
4129·74	1	0·96	4·35	4·21	4·12	4·73
4205·05	25	0·71	4·48	4·47	4·31	4·84
Gd II						
4215·02	32	0·44	4·98	4·73	4·88	5·40
4251·74	15	0·00	4·85	4·77	4·68	5·27

that the variation of $\rho\kappa$ is at best by a factor of ten over the cycle of pulsation. This is in marked contrast to values derived for κ Pav (Rodgers & Bell 1963) and SV Vul (Kraft, Camp, Fernie, Fujita & Hughes 1959). On the other hand it resembles closely the amplitude change of $\rho\kappa$ measured for η Aql (Schwarzschild, Schwarzschild & Adams 1948).

A second hump in log $\rho\kappa$ is seen at phase 0·68 P. An irregularity in the smooth variation of log P_e at this phase may explain in our opinion only part of the enhancement. A similar feature is seen for both κ Pav and SV Vul, though it is of much greater magnitude than is encountered in RT Aurigae. There is little similarity between the log $\rho\kappa$ curve and those of velocity and displacement. The half widths of the lines at phase 0·68 P are also noticeably larger than at phase 0·4 P. Presumably this indicates the sudden onset of the compression phase of the pulsation.

Both θ_{exc} and log P_e curves show a steep fall to a minimum value soon after phase 0·0 P, followed by a gradual rise to maximum. This is a pattern of change that differs from the visual light curve especially in the range of phase 0·0–0·2 P after light maximum.

6. *An estimate of the abundances.* Following Helfer, Wallerstein & Greenstein (1959) we have

$$[N_{\text{Fe I}}] = \left[\frac{N_{\text{Fe I}}}{\kappa V}\right] + [V] + [\kappa].$$

With information available on [Fe II/Fe I] and $[N_{\text{Fe I}}]$ we can readily evaluate $[N_{\text{Fe}}]$. We have attempted to determine abundances of RT Aurigae from the four spectra obtained with the 73-in. camera. The measured log W/λ values for any ion were entered into the corresponding curve of growth to give log η_*. The

TABLE VI

Atmospheric parameters

Plate	Ce 7970	Ce 7700	Ce 7655a	Ce 8329	Ce 8313	Ce 7532	Ce 8319	Ce 7969a	Ce 7996	Ce 7546	Ce 8323
Phase	0·024	0·046	0·107	0·215	0·414	0·565	0·680	0·750	0·825	0·861	0·946
θ_{exc}	0·94	0·99	1·03	1·04	1·05	1·07	1·06	1·04	1·04	0·99	0·97
θ_{ion}	0·79	0·84	0·88	0·89	0·90	0·92	0·91	0·89	0·89	0·84	0·82
log P_e	+0·33	−0·22	−0·43	−0·48	−0·51	−0·64	−0·32	−0·48	−0·13	−0·08	+0·03
$\log\frac{\text{Fe II}}{\text{Fe I}}$	2·88	2·97	2·82	2·81	2·72	2·67	2·43	2·43	2·78	2·84	2·90
$[\kappa]$	−1·11	−1·55	−1·73	−1·76	−1·78	−1·87	−1·58	−1·76	−1·43	−1·44	−1·35
log P_g	2·45	2·07	2·17	2·20	2·27	2·28	2·78	2·32	2·20	2·31	2·27
log $\rho\kappa$	−10·22	−11·06	−11·10	−11·09	−11·04	−11·11	−10·32	−10·97	−10·76	−10·69	−10·65
V (km s^{-1})	3·78	2·12	3·78	3·57	3·78	2·83	5·33	4·54	5·33	4·24	2·83
log a	−2·6	−3·0	−3·0	−3·0	−3·4	−3·0	−3·4	−3·4	−3·4	−2·6	−2·6
$[N_{Fe}]$	+0·30	−0·19	−0·36	−0·19	−0·08	−0·51	−0·19	−0·34	−0·06	−0·16	−0·30

TABLE VII

Mean abundances relative to [Fe]

Element	Process	[N]	No. of lines	Mean deviation
Mg	α, s	−0·18	18	0·22
Si	α, $s(m)$	−1·41	4	0·12
Ca	α, s	+0·18	36	0·17
Sc	s	−0·58	32	0·14
Ti	α, s, e, r	−0·22	117	0·09
V	e, (m)	−0·95	43	0·03
Cr	(e)	−0·48	64	0·13
Mn	(e)	−0·53	24	0·08
Fe	(e)	0	278	—
Co	(e)	−0·31	12	0·20
Ni	(e)	−0·46	25	0·12
Sr	$s(m)$	−0·25	8	0·11
Y	$s(m)$	+0·16	12	0·16
Zr	s	−0·72	35	0·04
Ba	s, r	−0·97	4	0·11
La	$s(m)$	−0·98	28	0·06
Ce	$s(m)$	−1·14	27	0·04
Pr	$s(m)$	−0·60	7	0·22
Nd	$s(m)$, s	−1·07	19	0·08
Sm	r, s	−0·56	12	0·10
Eu	r, s	−0·22	8	0·29
Gd	r, s	−1·11	8	0·05
Mean abundance	α, s	−0·03	58	—
	s	−0·71	149	—
	e	−0·15	403	—

shift Δ where,

$$\Delta = \log \eta_* - \log \eta_\odot - \chi(\theta_{\mathrm{exc}}{}^\odot - \theta_{\mathrm{exc}}{}^*)$$

gives $[N_{\mathrm{ion}}/N_{\mathrm{Fe\ I}}]$. We then have

$$\left[\frac{N_{\mathrm{ion}}}{N_{\mathrm{Fe}}}\right] = \left[\frac{N_{\mathrm{ion}}}{N_{\mathrm{Fe\ I}}}\right] + \left[\frac{N_{\mathrm{Fe\ I}}}{N_{\mathrm{Fe}}}\right].$$

For each ion a mean value of $[N_{\mathrm{ion}}/N_{\mathrm{Fe}}]$ for each phase was determined and this along with Saha's equation and the appropriate partition functions (Corliss 1962) give the relative abundance of the element with respect to iron.

We give in Table VI the value of $[N_{\mathrm{Fe}}]$ obtained for the 11 phases studied. The mean value is −0·21 and the standard error is ±0·15. We, therefore, conclude that there is little noticeable difference in the iron ratio between the cepheid and the Sun. In Table VII, the weighted mean of the derived abundances $[N_{\mathrm{el}}/N_{\mathrm{Fe}}]$ is shown; the weights are proportional to the number of lines measured. The deviations listed are the average residuals for each plate from the mean abundance. In cases where $[N_{\mathrm{el}}/N_{\mathrm{Fe}}]$ was available from more than one ion of the same element, the abundance values derived from each were averaged with appropriate weightage. The mean abundances, weighted on the basis of number of lines measured, determined separately for the α, s; e and s-process elements, are given at the bottom of the table. We notice that the s-process elements are

deficient with respect to the *e*-process elements by a factor of 3·5. The elements Mg, Ca, Ti have normal abundances. The case of deficient silicon is surprising. The abundance determination is only from one line and is likely to be very uncertain even though the values derived from the four phases are mutually consistent. Scandium is slightly underabundant and one thereby infers that since the *s*-process is responsible for its synthesis, the original stock of Ca^{40} must have been meagre. Most of the Ca^{40} now seen was probably formed subsequently. Among the iron peak elements V shows a striking underabundance. In this group Mn also exhibits appreciable deficiency. These low abundances must necessarily be considered as quite significant and would reflect the physical conditions under which the *e*-process was operative. The *s*-process elements are in general quite underabundant, the deficiency being of the order of 5 or greater from Zr through Nd. The Sr and Y to Zr ratio is noticeably strange even if one considers the low reliability of the Sr and Y abundances. Possibly the commencement of the deficiencies from Zr are related to the availability of large neutron fluxes required for heavy element synthesis by the *s*-process. The Eu abundance even though determined from two lines can be considered as normal.

These deficiencies in a disk population star of age $\simeq 10^8$ years are of interest from the standpoint of stellar nucleogenesis, specially in the case of a star that currently occupies the cepheid instability strip.

7. *The mass of RT Aurigae.* Fernie (1965) has derived a mass–period relation for classical cepheids which yields for RT Aurigae $\mathcal{M}/\mathcal{M}_\odot = 5{\cdot}7$. We have found the radius of the cepheid to be $33{\cdot}7\ R_\odot$. Fernie's relation (1968) indicates that RT Aurigae is most likely pulsating in its fundamental mode. Following Iben (1967) who gives the evolutionary track for a $5M_\odot$ star of Population I, we see that RT Aurigae is currently experiencing a second crossing of the cepheid instability strip. The star must have taken nearly 10^8 years to reach its present evolutionary state from the main sequence. In reaching this conclusion one has to assume that no serious mass-loss has occurred and that the evolutionary track is one for a star of constant mass.

Astrophysical Observatory,
Kodaikanal,
India.
1968 *August.*

Acknowledgments. The observations reported here were obtained by one of us (M. K. V. B.) while a Carnegie Fellow at the Mount Wilson and Palomar Observatories. We are indebted to K. K. Scaria for much help in the reductions.

References

Abt, H. A., 1960. *Astrophys. J.*, **131**, 99.
Aller, L. H., 1953. *Astrophysics*, Vol. 1, Ronald Press, New York, p. 291.
Aller, L. H., 1963. *Astrophysics*, Vol. 1, Ronald Press, New York, p. 129.
Bennett, A., 1941. *Astrophys. J.*, **93**, 52.
Corlis, C. H., 1962. *J. Res. natn. Bur. Stand.*, **66A**, 169.
Duncan, J. C., 1908. *Lick Obs. Bull.*, **5**, 81.
Eggen, O. J., Gascoigne, S. C. B. & Burr, E. J., 1957. *Mon. Not. R. astr. Soc.*, **117**, 406.
Fernie, J. D., 1965. *Astrophys. J.*, **142**, 1072.
Fernie, J. D., 1968. *Astrophys. J.*, **151**, 197.

Gingerich, O., 1962. Doctoral thesis, Harvard University.
Greenstein, J. L., 1948. *Astrophys. J.*, **107**, 141.
Helfer, H. L., Wallerstein, G. & Greenstein, J. L., 1959. *Astrophys. J.*, **129**, 700.
Iben, I. Jr., 1967. *Ann. Rev. Astr. Astrophys.*, **5**, 571.
Kraft, R. P., Camp, D. C., Fernie, J. D., Fujita, C. & Hughes, W. T., 1959. *Astrophys. J.*, **129**, 50.
Kukarkin, B., 1935. *Perem. Zvezdȳ*, **4**, 385.
Mitchell, S., 1930. *Astrophys. J.*, **71**, 1.
Petrie, R. M., 1932. *Publs Obs. Univ. Michigan*, **5**, 9.
Rodgers, A. W. & Bell, R. A., 1963. *Mon. Not. R. astr. Soc.*, **125**, 487.
Schwarzschild, M., Schwarzschild, B. & Adams, W. S., 1948. *Astrophys. J.*, **108**, 207.
Wesselink, A. J., 1946. *Bull. astr. Insts Neth.*, **10**, 91.
Wrubel, M. H., 1949. *Astrophys. J.*, **109**, 66.